

NdFeB Magnets with Well-Pronounced Anisotropic Magnetic Properties Made by Electric Current-Assisted Sintering

Tarini Prasad Mishra, Lennart Leich, Martin Krengel, Sebastian Weber, Arne Röttger, and Martin Bram*

Electric current-assisted sintering (ECAS) technologies are highly promising for processing of NdFeB magnets. Due to the combination of direct Joule heating and application of external load, even powders, whose particle size distribution and morphology are not optimum for conventional powder processing like melt-spun powders or magnet scrap, can be easily sintered to high densities. A systematic study is done to demonstrate the potential of field-assisted sintering technique/spark plasma sintering (FAST/SPS) and flash spark plasma sintering (flash SPS) for sintering of NdFeB powders. Melt-spun, commercial NdFeB powder (Magnequench MQU-F) is used as starting material. Its platelet-like shape makes this powder extremely difficult to sinter by conventional methods. This study clearly reveals that especially in the case of flash SPS application of external pressure in combination with short cycle times enables to achieve well-pronounced anisotropic magnetic properties without the need of subsequent upset forging. Optimized flash SPS parameters are applied to NdFeB magnet scrap with broad particle size distribution, demonstrating the general potential of ECAS technologies for recycling of waste magnet materials. Finally, the results are benchmarked with respect to established NdFeB processing technologies and electrodischarge sintering (EDS), another promising ECAS technology with very short cycling time.


their superior energy product $(BH)_{\max}$ (theoretical 512 kJ m^{-3}) compared with other permanent magnetic materials. Fine tuning of magnetic properties is achieved by tailoring the alloy composition with further heavy rare-earth elements (REEs) like Dy, Te, or Gd in combination with sophisticated material processing methods.^[1] NdFeB magnets are applied on a large scale in generators for wind turbines, electric vehicles, hybrid electric vehicles, E-bikes, consumer electronics, computers, and other green energy technologies.^[2–4] In 2015, global production of these kinds of magnets was around 60 000 tons. Chinese companies currently dominate the market due to geopolitical reasons.^[5] The amount of NdFeB magnets required for the operation of these devices varies between a few grams in the case of consumer electronics, several kilograms for electric vehicles, and up to tons for generators in wind turbines.^[6] According to the different life cycles of the devices, NdFeB magnets are usually operated between 2 and 3 years in consumer

electronics and up to 30 years in large generators. With respect to the significantly increasing need of high-performing permanent magnets and geopolitical limited availability of REEs,^[7] the following challenges exist to meet the future needs.

1. Introduction

Hard magnets on the basis of NdFeB with $\text{Nd}_2\text{Fe}_{14}\text{B}$ as the main phase play a vital role for the success of “Energiewende,” due to

T. Prasad Mishra, M. Bram
Institute of Energy and Climate Research
IEK-1: Material Synthesis and Processing
Forschungszentrum Jülich
Wilhelm-Johnen-Strasse, 52425 Jülich, Germany
E-mail: m.bram@fz-juelich.de

 The ORCID identification number(s) for the author(s) of this article can be found under <https://doi.org/10.1002/adem.202201027>.

© 2022 The Authors. Advanced Engineering Materials published by Wiley-VCH GmbH. This is an open access article under the terms of the Creative Commons Attribution-NonCommercial-NoDerivs License, which permits use and distribution in any medium, provided the original work is properly cited, the use is non-commercial and no modifications or adaptations are made.

DOI: 10.1002/adem.202201027

L. Leich, S. Weber
Institut für Werkstoffe
Lehrstuhl Werkstofftechnik
Ruhr Universität Bochum
Universitätsstraße 150, 44801 Bochum, Germany

M. Krengel
Magnetprototyping & Development Magnetic Materials
Wilo SE
WILO Park 1, 44263 Dortmund, Germany

A. Röttger
Lehrstuhl für Neue Fertigungstechnologien und Werkstoffe
Bergische Universität Wuppertal
Bahnhofstraße 15, 422651 Solingen, Germany

1.1. Development of Effective Recycling Strategies

Currently, there are no established technologies for effective recycling of NdFeB magnets. This is caused by the fact that production from primary sources is still the most economical way. Nevertheless, REE crisis in 2011^[8] and forecast of future supply shortages^[7] initiated large national and international projects to face the increasing supply risk. As example, European project SUSMAGPRO demonstrates which hurdles exist to effectively separate and recycle magnets at their end-of-life (EOL).^[5] Even if the need of an effective circular economy for REE containing materials is obvious, there is still large economical risk for stakeholders to invest in such technologies. Among others this is caused by the fact that—even if suitable recycling routes already exist—EOL magnets appear in a broad variety of alloying systems (e.g., SmCo, Ferrites, and NdFeB) and specific microstructures (sintered, polymer bonded, functionally coated, and others), making an effective separation and reliable identification of the material quite challenging. In addition, the overall amount of magnetic material especially in consumer electronics is rather low, further aggravating its effective separation.

Recycling strategies for NdFeB EOL magnets comprehend direct alloy production methods as well as metallurgical extraction and recovery methods. In the first case, NdFeB magnet scrap is either diminished into a powder by hydrogen decipitation with subsequent milling^[9,10] or recast into a master alloy by induction melting with subsequent melt spinning. In both cases, powders can be converted back to NdFeB magnets by applying conventional primary processing technologies. As alternative, hydrogenation disproportionation desorption and recombination (HDDR) are established processes to manufacture resin-bonded magnets from scrap materials.^[11,12]

1.2. Development of NdFeB Magnets Without or With Reduced Amount of Heavy REE

As an effective circular economy does not exist so far, avoiding or at least clearly reducing the amount of heavy REE in NdFeB magnets is an attractive alternative, at least as an intermediate solution. Therefore, development of new or optimized processing technologies is required to maintain magnetic properties competitive to magnets alloyed with heavy REEs, for example, by special tuning of microstructure.

1.3. Development of New Processing Technologies for NdFeB Magnets Aiming to Improve Magnetic Properties and to Increase Efficiency of Magnet Production

If aiming for magnets with superior magnetic properties, expensive and energy-intensive processing routes are the state of the art. NdFeB magnets with anisotropic magnetic properties can be either achieved by magnetic pulse alignment and compaction of microcrystalline NdFeB powders with subsequent sintering at high temperatures above 1000 °C.^[6,13] As an alternative, hot pressing of melt-spun NdFeB powders (temperature ≈650 °C and pressure ≈300 MPa) followed by hot deformation (temperature 650–750 °C and height reduction ≈50%) via die-upset forging or back extrusion is done.^[14,15] Conventionally,

sintering of compacts at high temperatures is usually coupled with strong grain growth, loss of anisotropy, and decrease in magnetic properties.^[16] Hot deformation techniques enable to maintain nanocrystalline grains staying below single-domain size of Nd₂Fe₁₄B phase (≈300 nm), which enhances coercivity, but sophisticated processing technology and expensive tooling lead to significantly enhanced processing costs.^[17,18] Furthermore, lower degree of texture compared with sintered magnets lowers the energy product (BH)_{max}.

On a lab scale, different electric current-assisted sintering (ECAS) technologies are already successfully applied for the production of NdFeB magnets with isotropic or even anisotropic magnetic properties. The following ECAS technologies have been investigated for NdFeB magnet production so far. Field-assisted sintering technology/spark plasma sintering (FAST/SPS) is a low-voltage, current-activated, and pressure-assisted sintering process, which is based on Joule heating of the conductive tools and characterized by high heating rates and short cycle times.^[19] In the case of NdFeB, direct Joule heating of the conductive powder supports the heat transfer from the tools. Ease of tool manufacturing especially when using graphite as tool material, short cycle times, densification near theoretical density, and retention of fine grain sizes leading to high coercivity motivate the application of FAST/SPS for magnet production in the lab. It is therefore described by many authors.^[16,20–24] Under conventional FAST/SPS conditions, isotropic properties still remain, making additional hot deformation of FAST/SPS samples necessary when aiming for anisotropic properties and high-energy products (BH)_{max}.^[25] Recently, Castle et al. demonstrated that flash SPS—a specific kind of operation mode possible in conventional FAST/SPS devices—might become an attractive alternative for processing of anisotropic NdFeB magnets with optimized energy product (BH)_{max}.^[25,26] In the flash SPS configuration, a precompacted or presintered NdFeB sample is placed between two graphite punches. A high-power current pulse of defined length (usually only a few seconds) is forced through the sample, which is additionally loaded by the punches. As such, flash SPS enables a simultaneous densification and hot deformation of the sample with large height reduction. Rapid nature of the process enables to retain nanoscale of grains and at the same time to produce crystallographic texture in the material. After process optimization, Castle et al. achieved an anisotropic magnet from Dy-free melt-spun NdFeB powder (Magnequench MQU-F) characterized by coercivity H_{ci} of 1438 kA m^{−1}, remanence B_r of 1.16 T, and energy product (BH)_{max} of 230 kJ m^{−3}. Recently, electrodischarge sintering (EDS)—also known as spark plasma consolidation (SPC)—was introduced by Leich et al. as another rapid and energy-saving ECAS process, which enables to even further reduce the processing time for compaction of NdFeB magnets to milliseconds.^[27–29] The potential of this technology for ultrarapid densification of NdFeB powders with comparatively low-energy demand^[29] was demonstrated on melt-spun powders (Magnequench MQU-F) and even on recycled powders produced by crushing and milling of EOL magnet scrap (formerly hot pressed, therefore, isotropic). Nevertheless, at current state of development, EDS microstructure still lacks homogeneity, exhibiting fully densified, partly densified, and remelted zones. Up to now, the best magnetic properties were achieved with magnets made from recycled

powder achieving a coercivity of 1083 kA m^{-1} , remanence of 0.84 T , and energy product $(BH)_{\text{max}}$ of 123 kJ m^{-3} .

Compared with established processing technologies mentioned before, ECAS technologies have the potential to further improve processing of NdFeB magnets and their magnetic properties due to the following hypotheses. Nevertheless, doubtless proof of these hypotheses still pends and requires further investigations.

- 1) Electroplasticity as additional deformation mechanism enables diameter-to-height ratios not accessible with established methods like die upsetting and decreases the required deformation load.^[30]
- 2) Decrease of deformation load reduces tool wear.
- 3) Direct Joule heating in combination with short dwell time and moderate load enables well-controlled anisotropic grain growth, while keeping the grain size below the domain size, which is one of the key factors for achieving pronounced anisotropic magnetic properties.
- 4) Exact microstructure control enables to reduce amount of heavy rare elements without loss of magnetic performance.^[26]
- 5) ECAS technologies have the potential to reduce cycle times and energy consumption, especially the EDS process.^[27–29]
- 6) ECAS technologies are suitable for direct densification of recycling powders made from magnetic scrap.

In the present work, a systematic experimental study was conducted to gain a better understanding of potentials and challenges when processing NdFeB magnets with anisotropic properties and maximum energy product $(BH)_{\text{max}}$ via FAST/SPS and flash SPS. For benchmarking our results with other processing technologies, Magnequench MQU-F powder was selected as starting material as same kind of powder was applied in the recent studies of Wüst et al. on FAST/SPS,^[16] Castle et al. on flash SPS,^[26] and Leich et al. on EDS.^[27,29] In our future work, optimized parameter sets will be the basis for the production of NdFeB magnets with tailored microstructures and well-defined magnetic properties starting from NdFeB powders with reduced amount of heavy rare metals as well as from recycle powders made of magnet scrap. Therefore, in a preliminary experiment, we applied flash SPS for the consolidation of NdFeB recycling powder, which was made by crushing and milling of die-upset magnets.

2. Experimental Section

2.1. Starting Powders

Commercial melt-spun NdFeB powder (MQU-F, Lot. B55557) from Magnequench was used as starting material. The powder had a typical ribbon-like morphology of melt-spun powders as for example shown in the work of Leich et al.^[27] The ribbons contained nanocrystalline grains with a size of about 50 nm . The nominal composition of the powder was $31.1\% \text{ Nb}$, $0.08\% \text{ Pr}$, $0.02\% \text{ Dy}$, $5.91\% \text{ Co}$, $0.54\% \text{ Ga}$, and $0.89\% \text{ B}$ (all values in wt%) and Fe as balance. In the alloy, Co replaces Fe for increasing the Currie temperature without significantly changing remanence and coercivity. Ga was added to improve the workability in the case of hot deformation. The recycled powder (LCM Batch J9348/FP33302 delivered by WILO) was produced by crushing and milling of hot-pressed magnets. Also in this case, MQU-F powder was applied as starting material for hot pressing. Nominal composition of this recycled powder was $30.0\%–31.2\% \text{ Nb}$, $0\% \text{ Pr}$, $<0.1 \text{ Dy}$, $6.0\%–6.5\% \text{ Co}$, $0.48\%–0.60\%$, and $0.88–0.94 \text{ B}$ (all values in wt%) and Fe as balance. **Figure 1** shows the morphologies of the MQU-F powder flakes and of the recycled REC-HP powder as well as the related particle size distributions. It must be noted that in both cases, the size of the primary grains in the nanometer range is much smaller than the measured particle size.

2.2. FAST/SPS of NdFeB Powder

FAST/SPS was performed in a HP-D 5 device (FCT Systeme GmbH, Rauenstein, Germany) in vacuum. The influence of sintering temperature on the densification behavior of the powders in FAST/SPS technique was studied by fabrication of pellets at different temperatures. Sample preparation was carried out by pouring 15 g of the starting powder into a graphite die (SGL Carbon, SIGRAFINE R7710) with an inner diameter of 20 mm . For improving the contact between tool components

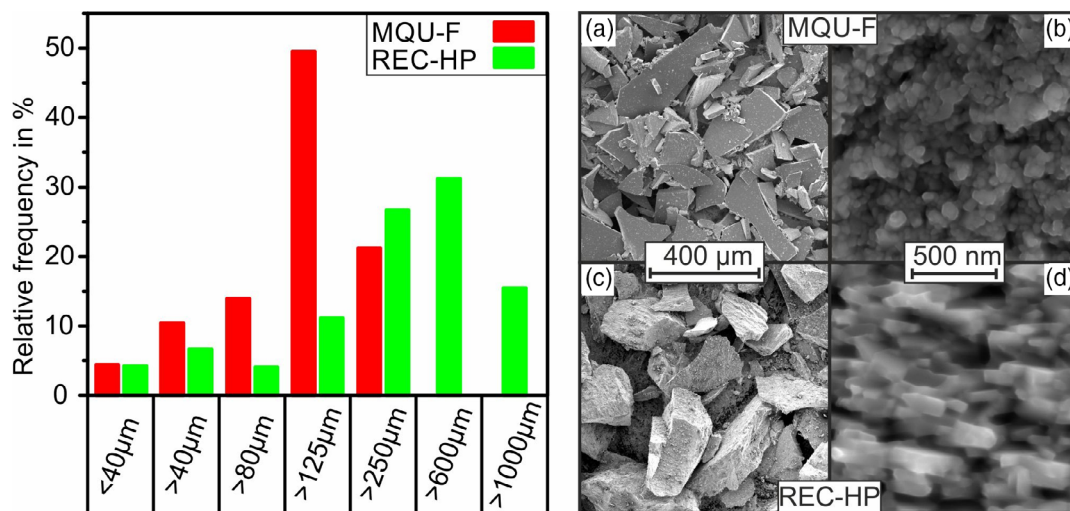


Figure 1. Particle size distribution (left) and powder morphology of the starting powders: a,b) MQU-F and c,d) REC-HP.

and sample, a graphite foil (SGL Carbon, SIGRAFEX) with a thickness of 0.35 mm was inserted. The pellets were heated to the respective sintering temperature (500, 600, 700, and 800 °C) with a heating rate of 100 K min⁻¹ followed by a dwell time of 30 s at the maximum temperature. A constant pressure of 50 MPa was applied throughout the whole sintering cycle. The processing parameters of the FAST/SPS samples were constant except the maximum sintering temperatures. Furthermore, all flash SPS samples were presintered by conventional FAST/SPS at 500 °C, which resulted in pellets with ≈73%–75% relative density. The presintering of the samples was found to be beneficial to enhance the stability of the compacts for mounting them in the flash SPS setup without damage, to withstand the minimum force of the FAST/SPS device of 10 kN uniformly applied in all flash SPS cycles and to ensure good electrical contact.

2.3. Flash SPS of Presintered NdFeB Pellets

All flash SPS cycles were conducted in a hybrid FAST/SPS device (H-HP-D 25 SD/FL/MoSi from FCT Systeme GmbH, Rauenstein, Germany). For conducting flash SPS, NdFeB pellets—presintered by FAST/SPS (100 K min⁻¹, 50 MPa, 500 °C, 30 s) with diameter of 20 mm, a height of ≈8 mm, and densities varying between 73% and 75% of the theoretical value—were placed between two graphite punches (diameter 60 mm) with plan parallel surfaces. Then a load of 10 kN (minimum load possible with the aforementioned FAST/SPS device, equivalent to 32 MPa for 20 mm samples) was applied to the samples. Samples were preheated to 300 °C via direct Joule heating with a maximum heating power of 8 kW. The limitation on the maximum heating power during preheating ensured a gradual increment of the sample temperature from room temperature to 300 °C. After a dwell time of 120 s, the samples were subjected to a pulse of continuous direct current systematically varying the maximum heating power and discharge duration, as detailed shown in Table 1. Two sets of experiments were conducted. In the first set, the maximum heating power was varied between 15 and 35 kW, while keeping the discharge time constant. In the second set, the discharge time was varied between 60 and 120 s at a constant maximum heating power of 20 kW. All cycles were conducted under a mild vacuum of

≈0.4 mbar. At the end of the power discharge, power was switched off and samples were cooled for 10 min in the equipment before opening of the chamber. For estimating the transferability of optimized flash SPS parameter sets for the densification of NdFeB recycle powders, sample preparation was repeated. As first step, recycled powders were presintered with 100 K min⁻¹, 50 MPa, 500 °C, 30 s, resulting in a relative density in the range of 67%–70% of the theoretical value. Afterward, two flash SPS cycles (REC-HP1_1, REC-HP1_2) were conducted using the parameters sets, as defined in Table 1.

2.4. Characterization

Particle size distribution was measured by sieve analysis. The density of the specimen was measured by the Archimedes principle. For density calculation, a theoretical density of 7.63 g cm⁻³ was used. For microstructure characterization, scanning electron microscopy (SEM) was conducted. Therefore, a TESCAN Mira 3 (Taipei, Taiwan) was operated in secondary electron (SE) mode and backscattered electron (BE) mode, using a working distance between 8 and 15 mm and an acceleration voltage of 15–20 kV. Before microstructure examination, samples were cut in two halves, one was used to prepare a cross section by grounding with 18 μm emery paper and subsequent polishing with water-free, 3 and 1 μm diamond suspensions. The other sample half was applied for measurement of magnetic properties using a Permagraph C-300 system (MAGNET-PHYSIK Dr. Steingroever GmbH, Köln, Germany) after previous magnetization in a pulsed field. A defined sample volume is necessary for magnetic characterization in the Permagraph. Due to a cracked edge area caused by the process, semicircular samples were eroded from the material.

3. Results and Discussions

In this section, the results on the densification of NdFeB magnets using FAST/SPS and flash SPS are discussed. This includes on the one hand characterization of the microstructure and on the other hand the determination of the magnetic properties. Results are benchmarked with NdFeB magnets processed by conventional methods (hot pressing, die-upsetting) and EDS. Finally, optimized parameter sets are applied for direct recycling of 100% magnetic scrap and preliminary results are discussed.

3.1. Processing of NdFeB Magnets by FAST/SPS and Flash SPS

Figure 2 summarizes the processing of NdFeB powders by two different electric field-assisted sintering technologies, that is, FAST/SPS and flash SPS. Figure 2a,b schematically shows the experimental setups for FAST/SPS and flash SPS used in the present investigation, respectively. In FAST/SPS process, the NdFeB powder is directly used for sintering, whereas, in flash SPS, the presintered pellet is used for densification. Presintering of the sample was found to be necessary to withstand the minimum load of 10 kN required for operation of the FAST/SPS device. With the simple flash SPS setup used in this study, it was not possible to produce near-net-shape NdFeB magnets, but only round magnets with a frayed edge area. Therefore, all samples for further characterization were cut from the center

Table 1. Overview of flash SPS samples produced for this study.

Sample code	Maximum power [kW]	Discharge time [s]
MQU-F1_1	15	30
MQU-F1_2	20	30
MQU-F1_3	25	30
MQU-F1_4	30	30
MQU-F1_5	35	30
MQU-F1_6	20	60
MQU-F1_7	20	90
MQU-F1_8	20	120
REC-HP1_1	35	30
REC-HP1_2	35	30

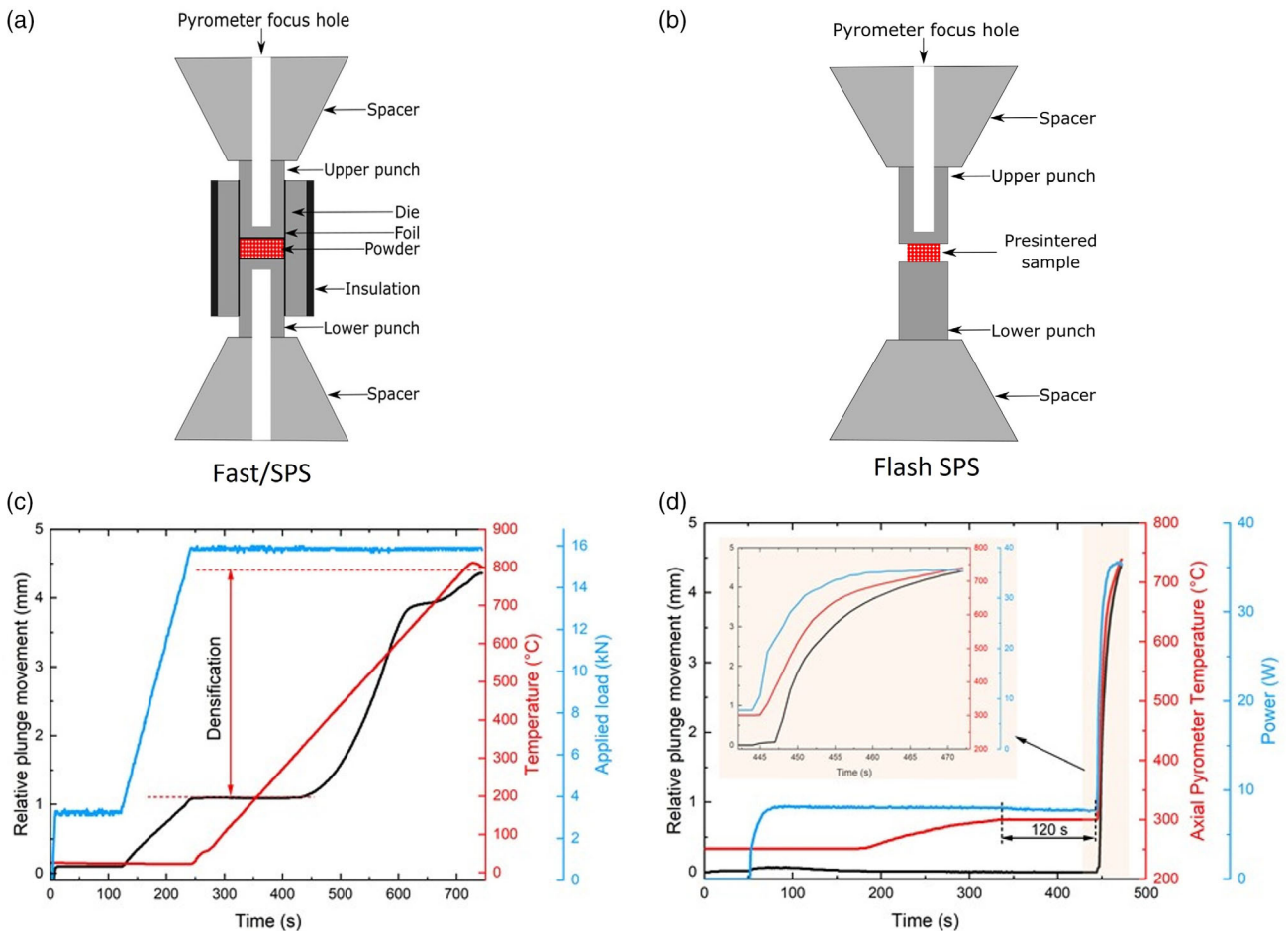


Figure 2. Schematic sketch of a) FAST/SPS setup and b) flash SPS setup. Processing parameters of the c) FAST/SPS cycle conducted with a maximum temperature of 800 °C and of the d) flash SPS cycle with a maximum power of 35 kW for 30 s.

of the flash SPS magnets. Figure 2c shows the processing parameters of a FAST/SPS cycle, where the sintering temperature was 800 °C. In other FAST/SPS cycles, only the maximum sintering temperature was varied, while all the other parameters were kept constant. During the FAST/SPS cycle, the sintering starts approximately at 450 °C. The black line in the diagram shows the relative movement of the punch as a function of temperature, which was influenced by the densification of the sample and the thermal expansion of the punches. Figure 2d shows the flash SPS cycle, where maximum power was set to 35 kW for 30 s. The inset plot shows the evolution of applied power, relative movement of the punch, and temperature measured by pyrometer during the 30 s dwell time. The flash SPS process can be divided into two steps. In step 1, a limited power of 8 kW was applied to heat the sample to 300 °C. After achieving the desired temperature of 300 °C, it was held for 120 s to ensure homogenous heating of the sample. In step 2, the maximum power was applied for 30 s. During the complete cycle, the minimum load possible with the equipment (10 kN) was applied to ensure a good electrical contact between the punch (electrodes) and the sample. It can be observed that the power supply required a specific time (≈ 12 s) to reach the defined maximum power. The black line shows the simultaneous deformation and densification of the sample.

The measured temperature values shown in the graph did not represent the actual sample temperature due to two reasons. On the one hand, the pyrometer focus was 5 mm above the sample. On the other hand, rapid increment of the sample temperature in very short time impeded exact temperature measurement.

Figure 3 exemplarily shows a sample presintered by FAST/SPS at 500 °C and a sample deformed by flash SPS with a maximum power of 35 kW for 30 s. In the case of flash SPS, the sample is frayed and several cracks are formed near to the edge due to conducting flash SPS without an outer die. To omit the influence of microstructural inhomogeneity on magnetic performance, the edge of all flash SPS samples had to be cut before measurement of magnetic properties, and therefore, magnetic properties are related to the center of the samples as already mentioned before.

Figure 4a shows the density of FAST/SPS samples as a function of sintering temperature. Almost fully dense pellets were achieved at sintering temperature of 700 °C. At higher temperatures, the densification of the powder saturated, which can be seen for the sample sintered at 800 °C. Figure 4b,c shows the density and deformation of flash SPS samples in axial and radial direction as a function of both power and total discharge time. In addition to the deformation, the deformation ratio φ can be calculated by Equation (1). Due to the less-defined geometry of



Figure 3. NdFeB samples after presintering by FAST/SPS (100 K min^{-1} , 50 MPa, 500 °C, 30 s) and after deformation by flash SPS (MQU-F1_5, 32 MPa, 35 kW, 30 s).

the sample edge, only the deformation ratio characterizing the height reduction was calculated.

$$\varphi_{\text{height}} = \ln\left(\frac{h_1}{h_0}\right) \quad (1)$$

For the first series of experiments with a constant dwell time of 30 s, φ_{height} was -0.15 , -0.31 , -0.55 , -0.78 , and -1.03 for heating power of 15, 20, 25, 30, and 35 kW. For the second series of experiments with constant heating power of 20 kW, φ_{height} was -0.31 , -0.51 , -0.68 , and -0.85 for a dwell time of 30, 60, 90, and 120 s.

In the current flash SPS setup, densification and deformation occurred simultaneously. Therefore, it is necessary to discuss both aspects together. The applied power in the flash SPS process clearly influences the degree of densification and deformation of the samples directly. In the present work, a maximum power of 35 kW is required to achieve a relative density of $\approx 97\%$. Furthermore, the sample was deformed 60% in the axial and 50% in the radial direction. Alternatively, the degree of densification can also be enhanced by limiting the maximum power and increasing the discharge time, as shown in Figure 4c. Here, the maximum power was limited to 20 kW and the discharge time was varied between 30 and 120 s. Similar degree of densification was achieved at 20 kW when the discharge time was increased to 120 s as compared with the sample that was sintered at a maximum power of 35 kW for 30 s. These results clearly evidence the

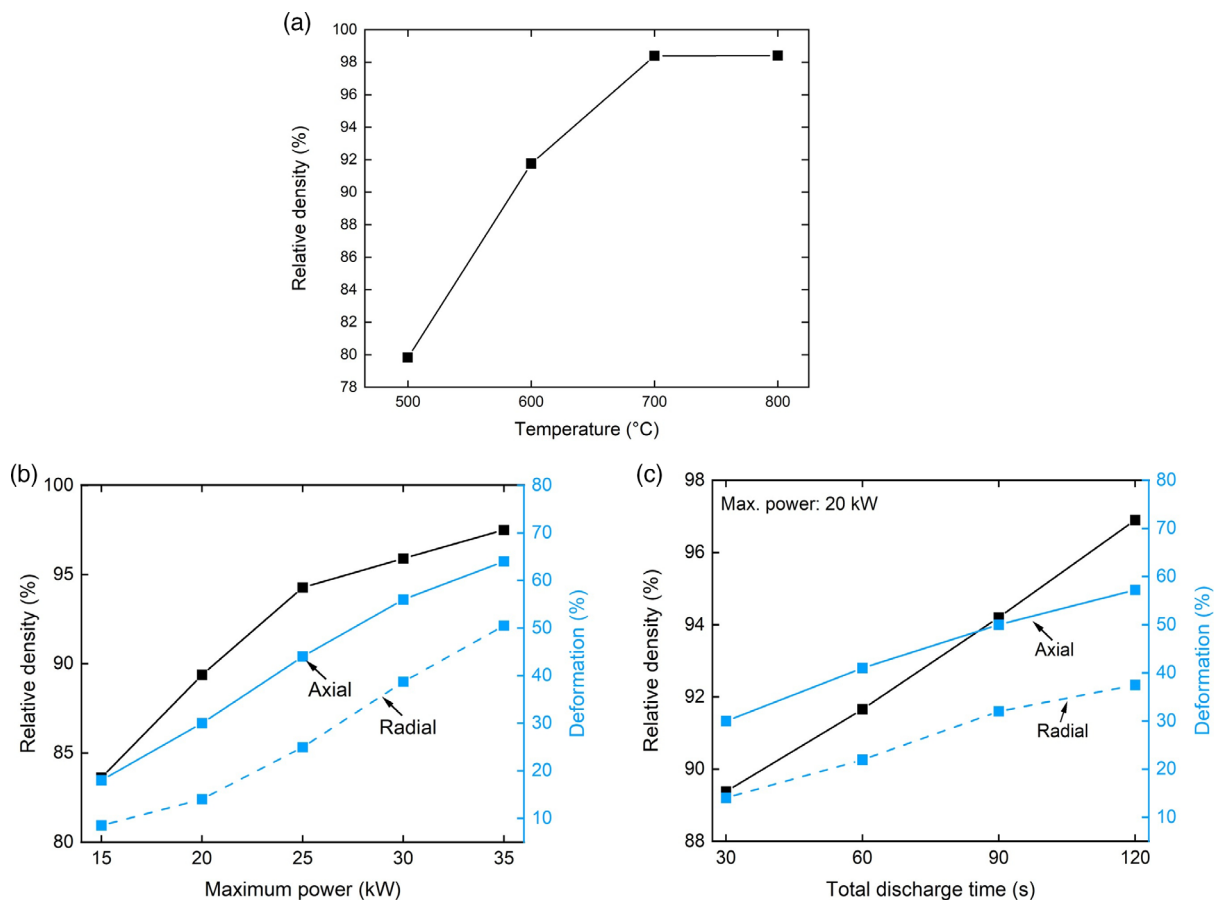


Figure 4. Densification of NdFeB material: a) as a function of temperature in FAST/SPS, b) as a function of power in flash SPS at a constant dwell time of 30 s, and c) as a function of dwell time in flash SPS at a constant power of 20 kW.

influence of maximum power and discharge time in the flash SPS process, which makes this process highly attractive for processing materials with controlled densification behavior and microstructure evolution.

The most striking result emerging from this study is that a deformation of 60% could be achieved at a mechanical pressure of mere 32 MPa in a short period of time. It is hard to draw sound conclusions on underlying deformation mechanisms without further investigations. Nevertheless, our hypothesis is that occurrence of electroplasticity effect^[30] might be the dominating effect to further improve magnetic properties when compared with conventional hot deformation. Furthermore, the possibility to conduct the flash SPS process with porous compacts enables almost maintaining the primary particle size until the deformation process starts. This might open new ways to realize anisotropic microstructures, which are difficult to achieve by established processing routes. More systematic parameter studies varying preheating temperature during flash SPS, applied pressure, and dwell time at maximum heating power are required to proof this hypothesis and understand the underlying deformation mechanisms better.

3.2. Microstructure of NdFeB Magnets by FAST/SPS and Flash SPS

Figure 5 shows the SEM micrographs of almost fully dense pellets sintered at 700 °C by FAST/SPS. The microstructure reveals a homogeneous distribution of nanosized and isotropic grains. The former powder particles are still visible, and grain coarsening can be seen at the powder particle transition points, which is due to a locally higher heat generation according to the Joule effect. With increasing temperature, the degree of densification (Figure 4a) as well as the grain coarsening increases. This kind of microstructure is representative for NdFeB magnets densified by FAST/SPS and is similar to other isotropic NdFeB magnets processed by, for example, EDS or hot pressing.

When aiming to achieve anisotropic grains, an additional hot-deformation step is necessarily required. In contrast,

samples densified by flash SPS directly reveal an anisotropic microstructure, provided suitable processing parameters are used. Figure 6 shows microstructures of four different samples, which were densified by flash SPS with varying parameters. A qualitative analysis of the microstructures indicates the much smaller grain size of the flash SPS samples when compared with the FAST/SPS samples, which were processed at 700 and 800 °C. It is supposed that this is mainly caused by the extremely high heating rate and the short dwell time in the case of flash SPS.

When sintered with a power of 20 and 25 kW, the grain morphology of flash SPS samples remains isotropic (Figure 6a,c). Further increase of power or discharge time resulted in the appearance of anisotropic, elongated, and coarsened grains, which are oriented perpendicular to the applied load. When increasing the power from 25 to 35 kW, the density was improved by merely 2%. In contrast, the deformation of the sample was increased by more than 10% in axial direction and more than 20% in radial direction. As a consequence, elongated and coarsened grains appear. Similarly, even when the maximum power was limited to 20 kW, the dwell time was increased from 30 to 120 s, and elongated and coarsened grains perpendicular to the applied load were achieved as well. These results clearly show that processing of NdFeB powders by flash SPS provides great opportunities not only for controlling the densification but also for tuning the microstructure by enhancing the degree of texture.^[31]

3.3. Benchmark of Magnetic Properties of Nanocrystalline NdFeB Magnets with Different Processing Technologies Starting from Melt-Spun MQU-F powder

In this section, the magnetic properties of nanocrystalline NdFeB magnets are discussed. First, the NdFeB magnets, which were densified by FAST/SPS and flash SPS in this study, are discussed and then a benchmark of the magnetic properties of conventionally densified as well as ECAS-densified NdFeB magnets is made.

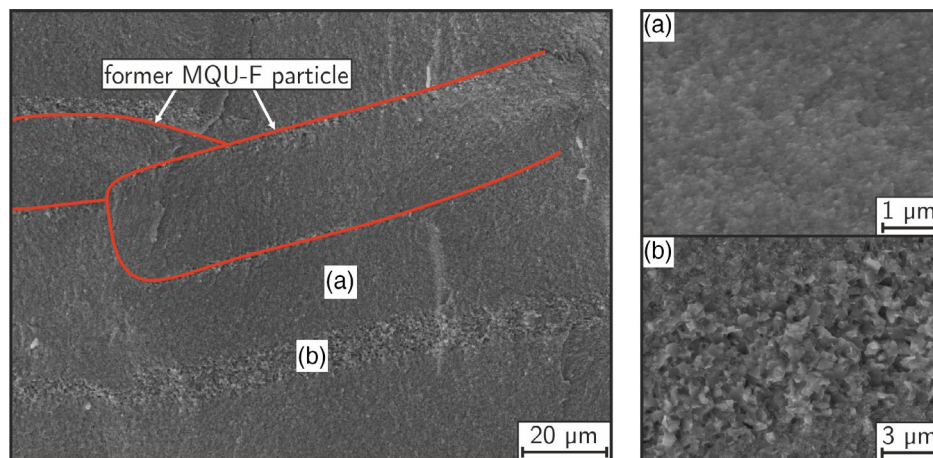


Figure 5. SEM micrographs showing typical microstructures of the pellets processed by FAST/SPS, sintered at 800 °C for 30 s, at heating rate 100 K min⁻¹, and an applied uniaxial pressure of 50 MPa.

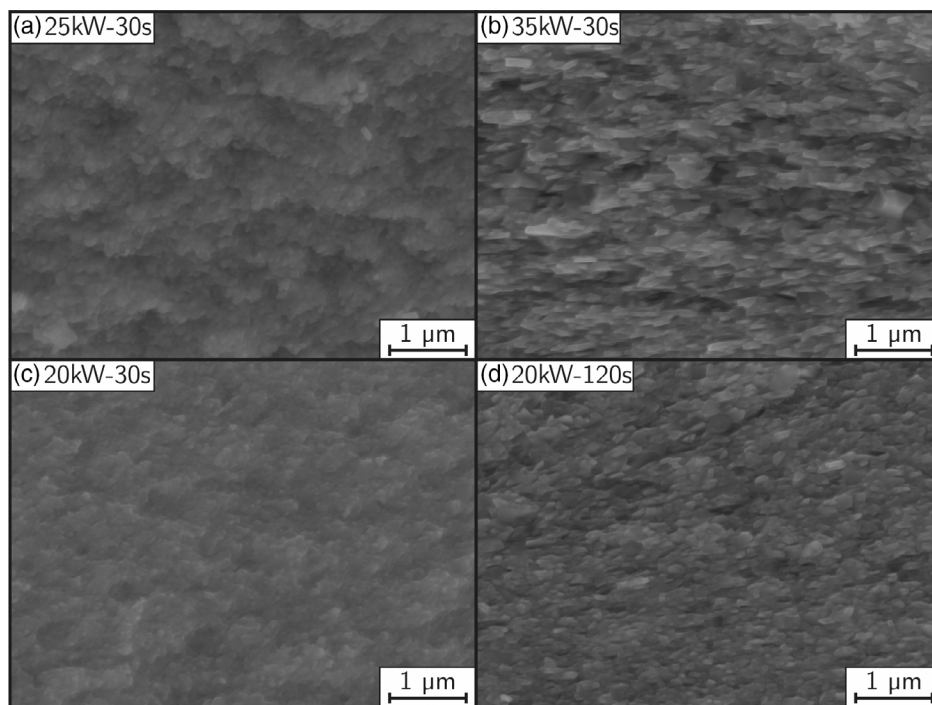


Figure 6. SEM micrographs of the fractured surface of pellets sintered via flash SPS: a) maximum power 35 kW for 30 s, b) maximum power 35 kW for 30 s, and c) maximum power 20 kW for 30 s and d) maximum power 20 kW for 120 s. A uniaxial pressure of 32 MPa was applied during the complete flash SPS cycle, which was conducted in vacuum (0.4 mbar).

3.3.1. Nanocrystalline NdFeB Magnets Processed by FAST/SPS and Flash SPS in This Study

Figure 7 shows the magnetic hysteresis curves for NdFeB magnets processed by FAST/SPS and flash SPS for different process parameters. During the FAST/SPS process, the process temperature was varied between 500 and 800 °C. At 500 and 600 °C, the remanence is reduced and below the theoretical maximum of isotropic NdFeB magnets of 0.8 T (Figure 7a), which can be attributed to lower sample densities (Figure 4a). At temperatures of 700 and 800 °C, the density of the specimen is increased and thus higher remanences, 0.84 and 0.85 T, were measured. The remanence is above the theoretical maximum of 0.8 T, which is due to slight texturing of the spherical nanocrystalline crystallites.

The coercivity is for the temperatures 500, 600, and 700 °C above 1650 kA m^{-1} , which indicates only a small and localized coarsening of the nanocrystalline grains. Only above 800 °C a decrease of the coercivity to 1269 kA m^{-1} can be measured and is due to a coarsened microstructure (Figure 5b). For the flash SPS process, presintered NdFeB magnets (FAST/SPS: 500 °C for 30 s, 100 K min^{-1}) were used. These specimens were densified via flash SPS on the one hand with varying power (Figure 7b) and on the other hand with varying the holding time at a constant power (Figure 7c). The exact values as well as the energy product are listed in **Table 2**.

In the current flash SPS setup, densification and deformation occurred simultaneously. Therefore, the increase of the remanence can be attributed on the one hand to an increase of the specimen's density and on the other hand to the formation of

elongated grains with a magnetic anisotropy. In this study, it was shown that both higher heating powers and longer dwell times led to an increase of the remanence, with the maximum remanence of 1.18 T being found at a heating power of 35 kW and a dwell time of 30 s. However, high heating powers (e.g., 35 kW) also led to grain coarsening and thus the coercivity is reduced from >1650 to 1483 kA m^{-1} . With a heating power of 20 kW for 120 s, the coercivity is only reduced to 1589 kA m^{-1} . Our best results for the FAST/SPS setup (700 °C, 100 K min^{-1} , 30 s, 50 MPa) are a coercivity H_{ci} of 1683 kA m^{-1} , a remanence B_r of 0.84 T, and a resulting magnetic energy product $(BH)_{\max}$ of 123 kJ m^{-3} . For the flash SPS setup (35 kW, 30 s, 32 MPa), a coercivity H_{ci} of 1483 kA m^{-1} , a remanence B_r of 1.18 T, and a resulting magnetic energy product $(BH)_{\max}$ of 264 kJ m^{-3} could be achieved.

3.3.2. Benchmark of Technologies to Produce Nanocrystalline NdFeB Magnets

In this section, the magnetic properties of NdFeB magnets processed will be compared with magnets made by EDS as well as conventional manufacturing routes (hot-pressing and die-upsetting). **Table 3** lists the coercivity H_{ci} in kA m^{-1} , remanence B_r in T, and the energy product $(BH)_{\max}$ in kJ m^{-3} of differently processed NdFeB magnets (EDS, hot-pressing, die-upsetting, flash SPS, and FAST/SPS). In general, a distinction can be made between processes with which anisotropic NdFeB magnets (die-upsetting, flash SPS) and processes with which isotropic NdFeB magnets (EDS, FAST/SPS, hot-pressing) can be produced. In a

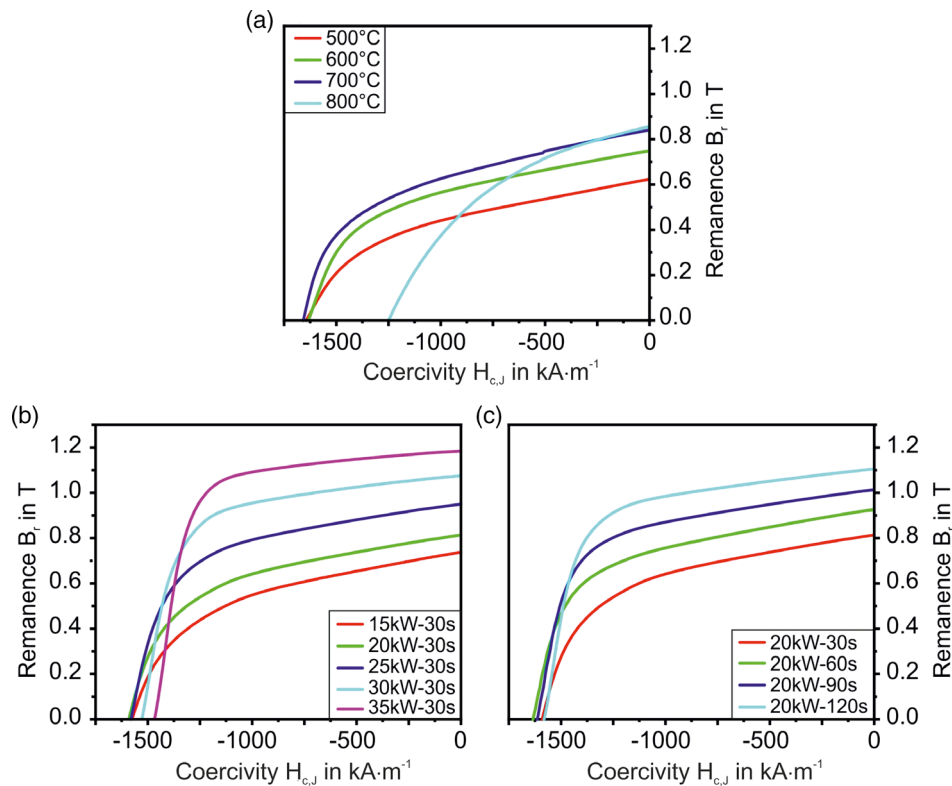


Figure 7. Magnetic hysteresis curves for the sintered NdFeB specimens at different processing parameters by a) FAST/SPS, b) flash SPS as a function of varied power for a discharge time of 30 s, and c) as a function of varied discharge time with maximum power of 20 kW.

Table 2. Coercivity H_{cJ} in kA m^{-1} , remanence B_r in T, and the energy product $(BH)_{\max}$ in kJ m^{-3} of NdFeB magnets processed by flash SPS with varying heating power and dwell time.

Flash SPS parameters	Coercivity H_{cJ} in $[\text{kA m}^{-1}]$	Remanence B_r in [T]	Energy product $(BH)_{\max}$ in $[\text{kJ m}^{-3}]$
15 kW/30 s	1590	0.74	96
20 kW/30 s	1606	0.81	118
25 kW/30 s	1596	0.95	162
30 kW/30 s	1544	1.07	213
35 kW/30 s	1483	1.18	264
20 kW/60 s	1642	0.93	152
20 kW/90 s	1621	1.01	186
20 kW/120 s	1589	1.10	224

Table 3. Coercivity H_{cJ} in kA m^{-1} , remanence B_r in T, and energy product $(BH)_{\max}$ in kJ m^{-3} of differently processed NdFeB magnets.

Process	Coercivity H_{cJ} in $[\text{kA m}^{-1}]$	Remanence B_r in [T]	Energy Product $(BH)_{\max}$ in $[\text{kJ m}^{-3}]$
EDS ^[27,29]	1565	0.78	102
Hot-pressing ^{a)}	1569	0.83	120
FAST/SPS	1683	0.84	123
Die-upsetting ^{a)}	1342	1.30	323
Flash SPS	1483	1.18	264

^{a)}WILO SE.

first step, the processes to densify isotropic NdFeB magnets will be compared.

Using both hot-pressing and FAST/SPS, the samples can be fully compacted and remanences of just above the isotropic maximum of 0.8 T are achieved. During hot pressing, a cold-pressed NdFeB magnet is placed in a minimally larger die, resulting in slight flow and thus slight magnetic anisotropy. In FAST/SPS, a similar slight flow of the spherical grains can be observed. In the EDS process, remanences slightly lower than 0.8 T are obtained, which is due to the process-related and unpreventable formation of insufficiently compacted as well as remelted microstructures,

which deteriorate the magnetic properties.^[27,29] Wüst et al. densified nanocrystalline NdFeB powders using FAST/SPS as well, but significantly higher compressive stresses (300 MPa) as well as longer holding times (7 min) were used in the study. Especially the longer holding time resulted in lower coercivity, which is due to coarsening processes as well as dissolution of the nanocrystalline phase $\text{Nd}_2\text{Fe}_{14}\text{B}$.^[16] Using flash SPS, it is possible to produce anisotropic nanocrystalline NdFeB magnets that approach the properties of conventionally produced anisotropic NdFeB magnets (die-upsetting). However, the anisotropic NdFeB magnets densified in this study have an energy product $(BH)_{\max}$ of 264 kJ m^{-3} , which is lower than conventional grades (323 kJ m^{-3}), see Table 3. Nevertheless, it is obvious from the

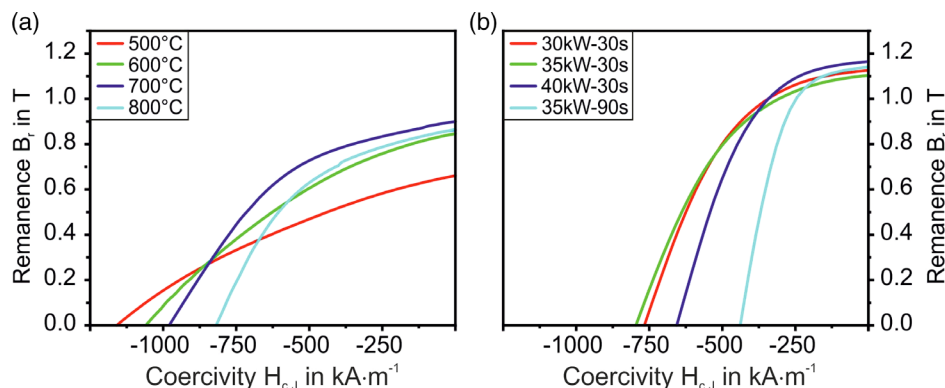


Figure 8. Magnetic hysteresis curves for the recycled NdFeB specimens with different processing parameters by a) FAST/SPS and b) flash SPS.

literature that even higher-energy products can be obtained when using a modified FAST/SPS setup for hot deformation. For example, Wang et al. processed nanocrystalline NdFeB powder to anisotropic NdFeB magnets with coercivity H_{ci} of 1234 kA m^{-1} , a remanence B_r of 1.42 T , and a resulting magnetic energy product $(BH)_{\max}$ of 385.9 kJ m^{-3} using a not-in-detail-specified FAST/SPS setup.^[32] In this context, the much higher compressive stresses (500 MPa) than those used in the present study (32 MPa) should be noted. Furthermore, the lower coercivity H_{ci} indicates higher process temperatures or longer holding times during the hot deformation process. Castle et al. used significantly lower compressive stresses in their flash SPS study, which were of the same order of magnitude as the compressive stresses used within this study and led to comparable magnetic properties.^[26]

The results obtained so far, as well as the state of the literature, show the potential of the flash SPS method for the fabrication of high-performance nanocrystalline NdFeB magnets and motivate further investigations.

3.4. Transfer of Results for Recycling of Hot-Pressed Magnets via FAST/SPS and Flash SPS

Another aspect of this study was to investigate the possibility of processing 100% magnetic scrap from old nanocrystalline anisotropic NdFeB magnets, which were produced by die-upsetting, into recycled NdFeB magnets using FAST/SPS and flash SPS. Figure 8 shows the magnetic hysteresis curves for NdFeB magnets made from recycling powder (REC-HP) processed by FAST/SPS and flash SPS for different process parameters. During the FAST/SPS process, the process temperature was varied between 500 and 800°C (Figure 8a).

For the flash SPS process, presintered NdFeB magnets (FAST/SPS: 500°C for 30 s , 100 K min^{-1}) were used and subsequently densified via flash SPS with varying power and holding time (Figure 8b). The exact values as well as the energy product are listed in Table 4. Compared with the NdFeB magnets out of MQU-F powder, the NdFeB magnets out of REC-HP powder possess a lower coercivity (see Table 2 and 4). The lower coercivity is due to the temperature load during the first processing (hot pressing and die upsetting), which leads to a coarsening of the nanocrystalline structure of the MQU-F particles and thus

Table 4. Coercivity H_{cj} in kA m^{-1} , remanence B_r in T , and energy product $(BH)_{\max}$ in kJ m^{-3} of recycled NdFeB magnets by FAST/SPS and flash SPS.

Process parameters	Coercivity H_{cj} in $[\text{kA m}^{-1}]$	Remanence B_r in $[\text{T}]$	Energy product $(BH)_{\max}$ in $[\text{kJ m}^{-3}]$
FAST/SPS— 500°C	1163	0.66	70
FAST/SPS— 600°C	1063	0.85	111
FAST/SPS— 700°C	983	0.90	132
FAST/SPS— 800°C	822	0.86	119
Flash SPS— $30 \text{ kW}/30 \text{ s}$	779	1.12	198
Flash SPS— $35 \text{ kW}/30 \text{ s}$	809	1.10	189
Flash SPS— $40 \text{ kW}/30 \text{ s}$	667	1.16	202
Flash SPS— $35 \text{ kW}/90 \text{ s}$	446	1.14	172

a decrease in coercivity. For FAST/SPS, the remanence B_r indicates an anisotropy that goes beyond a slight press anisotropy. Here, it must be investigated whether the anisotropy is caused by alignment of the powder particles of the broken magnets or by an alignment of the grains due to the current flow or other process parameters. For flash SPS, the remanence B_r and thus the alignment is better at higher heating powers or longer holding times.

4. Conclusions and Outlook

We have shown that it is possible to densify nanocrystalline NdFeB powder to achieve fully dense isotropic and anisotropic magnets with good magnetic properties using FAST/SPS and flash SPS. The key results are as follows: 1) In this study, isotropic NdFeB magnets densified by FAST/SPS (best parameters: 700°C , 100 K min^{-1} , 30 s , 50 MPa) have a coercivity of $>1600 \text{ kA m}^{-1}$ and a remanence of up to 0.84 T , indicating low magnetic anisotropy. 2) The microstructure of NdFeB magnets densified by FAST/SPS consists of spherical nanocrystalline grains. When using too high temperatures (800°C), the nanocrystalline structure significantly coarsened, especially at the powder particle transition points. 3) In this study, anisotropic NdFeB magnets densified by flash SPS (best parameters:

35 kW, 30 s, 32 MPa) that have a coercivity of $>1450 \text{ kA m}^{-1}$ and a remanence of up to 1.18 T. 4) The microstructure of NdFeB magnets consists of elongated, coarsened nanocrystalline grains, which are oriented perpendicular to the applied load. Higher heating powers and holding times lead to an increased flow of the grains and thus magnetic anisotropy.

The results presented in this work are the basis for the ongoing development of FAST/SPS and flash SPS technology for processing of NdFeB magnets in the framework of the GENESIS project. On the one hand, we are working on further optimization of the flash SPS technology for fine tuning the microstructure with respect to grain size, grain anisotropy, and interface between the grains. On the other hand, scale up of the technology and production of net-shaped magnets with large diameter-to-height ratio are open tasks. Last not least, application of FAST/SPS and flash SPS for recycling of magnet scrap is of high relevance with respect to the “Energiewende.”

Acknowledgements

Part of this work was supported by the German Research Foundation (DFG) within the Priority Program “Manipulation of matter controlled by an electric and magnetic field” (SPP 1959) under the grant number BR 3418/1-2. In addition, ongoing work was funded by German Federal Ministry for Economic Affairs and Climate Action (BMWK) according to a decision of the German Federal Parliament in the framework of the project “GENESIS—EnerGieeffizIENTE Kreislaufwirtschaft kritischer Rohstoffe,” Förderkennzeichen 03EI5009D. Funding is highly acknowledged. Experimental support and fruitful discussions of Ralf Steinert, Dr. Hans Peter Buchkremer, and Dr. Moritz Kindelmann are highly acknowledged.

Open Access funding enabled and organized by Projekt DEAL.

Conflict of Interest

The authors declare no conflict of interest.

Data Availability Statement

The data that support the findings of this study are available from the corresponding author upon reasonable request.

Keywords

anisotropic magnetic properties, field-assisted sintering technology/spark plasma sintering, flash spark plasma sintering, NdFeB magnets, recycling

Received: July 15, 2022

Revised: September 22, 2022

Published online: October 6, 2022

- [1] E. Alonso, A. M. Sherman, T. J. Wallington, M. P. Everson, R. Field, R. Roth, R. E. Kirchain, *Environ. Sci. Technol.* **2021**, *46*, 3406.
- [2] O. Gutfleisch, M. A. Willard, E. Brück, C. H. Chen, S. G. Sankar, J. Ping Liu, *Adv. Mater.* **2011**, *23*, 821.
- [3] Y. Matsuura, *J. Magn. Magn. Mater.* **2006**, *303*, 344.

- [4] S. Sugimoto, *J. Phys. D: Appl. Phys.* **2011**, *44*, 64001.
- [5] C. Burckhardt, presented at *EPMA Functional Materials Online Seminar, Functional Materials for Energy*, San Sebastian, Spain, June 01–June 02, 2021.
- [6] Y. Yang, A. Walton, R. Sheridan, K. Güth, R. Gauß, O. Gutfleisch, M. Buchert, B.-M. Steenari, T. Van Gerven, P. T. Jones, K. Binnemanns, *J. Sustainable Metall.* **2017**, *3*, 122.
- [7] J. H. Rademaker, R. Kleijn, Y. Yang, *Environ. Sci. Technol.* **2013**, *47*, 10129.
- [8] K. Bourzac, *Technol. Rev.* **2011**, *114*, 58.
- [9] M. Zakotnik, I. R. Harris, A. J. Williams, *J. Alloys Compd.* **2008**, *450*, 525.
- [10] M. Zakotnik, C. O. Tudor, *Waste Manage.* **2015**, *44*, 48.
- [11] O. Gutfleisch, K. Güth, T. G. Woodcock, L. Schultz, *Adv. Energy Mater.* **2013**, *3*, 151.
- [12] R. S. Sheridan, R. Sillitoe, M. Zakotnik, A. J. Williams, *J. Magn. Magn. Mater.* **2012**, *324*, 63.
- [13] O. Gutfleisch, *J. Phys. D* **200**, R157.
- [14] J. Song, M. Yue, J. Zuo, Z. Zhang, W. Liu, D. Zhang, J. Zhang, Z. Guo, W. Li, *J. Rare Earths* **2013**, *31*, 674.
- [15] J. J. Croat, *Rapidly Solidified Neodymium-Iron-Boron Permanent Magnets*, Woodhead Publishing Series in Electronic and Optical Materials, Elsevier, Woodhead Publishing, Duxford, UK **2018**.
- [16] Y. Yang, A. Walton, R. Sheridan, K. Güth, R. Gauß, O. Gutfleisch, M. Buchert, B.-M. Steenari, T. Van Gerven, P. T. Jones, K. Binnemanns, *J. Sustainable Metall.* **2017**, *3*, 122.
- [17] O. Gutfleisch, A. Kirchner, W. Grünberger, D. Hinz, H. Nagel, P. Thompson, J. N. Chapman, K. H. Müller, I. R. Harris, L. Schultz, *J. Phys. D* **1998**, *31*, 807.
- [18] I. Dirba, S. Sawatzki, O. Gutfleisch, *J. Alloys Compd.* **2014**, *589*, 301.
- [19] O. Guillon, J. Gonzalez-Julian, B. Dargatz, T. Kessel, G. Schierning, J. Räthel, M. Hermann, *Adv. Eng. Mater.* **2014**, *16*, 830.
- [20] M. Yue, J. Zhang, M. Tian, *J. Appl. Phys.* **2006**, *99*, 08B502.
- [21] M. Yue, A. Cao, G. Wang, W. Liu, J. Zhang, *Phys. Status Solidi A* **2007**, *204*, 4149.
- [22] W. Q. Liu, Z. Z. Cui, X. F. Yi, M. Yue, Y. B. Jiang, D. T. Zhang, J. X. Zhang, X. B. Liu, *J. Appl. Phys.* **2010**, *107*, 09A719.
- [23] Y. L. Huang, Z. W. Liu, X. C. Zhong, H. Y. Du, D. C. Zeng, *Powder Metall.* **2012**, *55*, 124.
- [24] W. Kaszuwara, M. Leonowicz, B. Michalski, M. Lis, *EPJ Web Conf.* **2013**, *40*, 06002.
- [25] E. Castle, S. Grasso, M. Reece, R. Sheridan, A. Walton, *J. Magn. Magn. Mater.* **2016**, *417*, 279.
- [26] E. Castle, R. Sheridan, W. Zhou, S. Grasso, A. Walton, M. J. Reece, *Sci. Rep.* **2017**, *7*, 11134.
- [27] L. Leich, A. Röttger, W. Theisen, M. Krengel, *J. Magn. Magn. Mater.* **2018**, *460*, 454.
- [28] L. Leich, A. Röttger, M. Krengel, W. Theisen, *J. Sustainable Metall.* **2019**, *5*, 107.
- [29] L. Leich, A. Röttger, R. Kuchenbecker, W. Theisen, *J. Mater. Sci.: Mater. Electron.* **2020**, *31*, 20431.
- [30] N. K. Dimitrov, Y. Liu, M. F. Horstemeyer, *Mech. Adv. Mater. Struct.* **2022**, *5*, 705.
- [31] D. Eckert, P. Nothnagel, K.-H. Müller, A. Handstein, *J. Magn. Magn. Mater.* **1991**, *101*, 385.
- [32] T. Wang, M. Yue, Y. Li, M. Tokita, Q. Wu, D. Zhang, J. Zhang, *IEEE Magn. Lett.* **2015**, *6*, 5500304.